Supporting Information

Boosting Photo-Induced Charge Separation by the NaV_2O_5/BiOCl Nanocomposite for Alkaline Water Splitting and Environmental Remediation

Soumita Sarkar, Soumalya Banerjee, Sk Afsar Ali, and Astam K. Patra*

Department of Chemistry, University of Kalyani, Kalyani, 741235, West Bengal, India.

*Corresponding author email E-mail: astamchem18@klyuniv.ac.in, Orcid.org/0000-0001-6071-8653.

Experimental details

Photoelectrochemical measurements

Electrode Preparation

The working electrode utilized in this experiment was the NaV_2O_5/BiOCl, NaV_2O_5 and BiOCl materials on Ni Foam (NF), with an electrolyte solution of 1 M KOH. The working electrode was made according to usual technique. To prepare materials supported on Ni foam, at first the Ni foams were cleaned with 1(M) HCl, DI water and acetone. 5 mg of the NaV_2O_5/BiOCl nanocomposite powder was then ultrasonically dispersed in 80 μL dry ethanol with 40 μL of Nafion (5%) solution for 1 h to obtain the catalyst ink. 100 μL of NaV_2O_5/BiOCl ink was drop-cast on NF (1×1 cm^2) and dried at ambient temperature to obtain NaV_2O_5/BiOCl electrode.

Electrochemical Characterization

The electrochemical properties were measured using computer-controlled electrochemical workstation (BioLogic 150e) system with techniques like CA, LSV, and chronopotentiometry. All the electrochemical experiments were carried out by employing a conventional three-electrode set-up, where a Pt wire and Ag/AgCl (in 3 M NaCl) were used as the counter electrode and reference, respectively. NaV_2O_5/BiOCl catalyst-loaded nickel foam (NF) electrode was used as the working electrode. The white light was provided by a 300 W Xe lamp (light intensity 100 mW/cm^2, photon flux 4.153 × 1017 cm^{-2} s^{-1}). The separation between the light source and the photoelectrochemical cell was 10 cm. Before beginning the experiments, argon gas was added to the solution. The chronoamperometry experiment was performed at 1.2 V bias with the chopping illumination method, in which the beam intensity was repeatedly turned on and off. The Mott−Schottky experiments were carried out with different frequencies in dark conditions to determine the flat-band potential. The perturbation signal for the analysis was set at 10 mV. The electrochemical impedance spectra (EIS) were recorded to find the charge transfer phenomena at the electrode−electrolyte interface at initial voltages of 0.8 V and -1.2V (V vs RHE) for the OER and HER studies, respectively with amplitude of 10 mV within the frequency range of 100 kHz–100 mHz. The equivalent circuit model was used to determine the solution resistance (R1) and charge transfer resistance (R2). Linear sweep voltammetry (LSV) measurements were conducted in Ar-saturated 1.0 M KOH at a scan rate of 5 mV s^{-1} from 1.0 to 2.0 V vs RHE for the OER and 0 to −0.9 V vs RHE for the HER. The iR compensation LSV was conducted manually, utilizing 85.0% of the impedance spectroscopy (EIS) R_1 values in both

light and dark conditions. In addition, the electrochemical performances of all NaV_2O_5, BiOCl electrodes, a bare NF were measured and compared. Chronopotentiometry was used to study the stability of the electrode materials. The applied potentials vs. Ag/AgCl (NaCl Sat'd) were converted to RHE (Reversible Hydrogen Electrode) potentials using the following equations:

$E_{RHE} = E_{Ag/AgCl} + 0.0591pH + E^{\theta}_{Ag/}$,where pH = 14 ($E^{\theta}_{Ag/AgCl}$= 0.194 V vs NHE at 25 °C)

Equation 1

Overpotential measurement

The overpotential values of all the catalysts were calculated at a benchmarking current density of 10 mA cm^{-2} for HER and and 50 mA cm^{-2} for OER by employing the following relation:

10 mA cm^{-2} (HER) = (0-E_{obs}) V versus RHE Equation 2

50 mA cm^{-2} (OER) = (E_{obs}-1.23) V versus RHE Equation 3

The Tafel Slope

The Tafel slope was calculated by fitting the overpotential versus log (j) using the Tafel equation as given below:

$\eta = a + b \times \log (j/j_0)$ Equation 4

where "b" signifies the Tafel slope value, "j" implies the current density value, and "j_0" is the exchange current density.

Electrochemical Active Surface Area (ECSA)

The electrochemically active surface area (ECSA) was analyzed from double-layer capacitance (C_{dl}) using cyclic voltammetry (CV) under different scan rates from 10 to 100 mV s^{-1}. The electrochemical active surface areas (ECSA) were measured by determining the electrochemical Cdl using the following equations:

$i_c = \nu \times C_{dl}$ Equation 5

$ECSA = C_{dl}/C_s$ equation 6

where "i_c" indicates the double-layer charging current resulting from scan-rates (ν) dependent CVs at non-faradic potential, and "C_s" denotes a specific capacitance value of 0.040 mF cm^{-2} depending on the typical reported values.

Characterization technique

The synthesized materials were analyzed using various characterization techniques. The powder X-ray diffraction patterns of the samples were obtained using a Bruker D-8 Advance diffractometer, operating at 40 kV voltage and 40 mA current, and utilizing Cu Ka radiation with a wavelength of 0.15406 nm. The Powder X-ray diffraction patterns were analyzed using EXPO2014 program and MATCH software, Version 3.x, by CRYSTAL IMPACT located at Kreuzherrenstr, 102, 53227 Bonn, Germany to determine the phase of the synthesized materials. Morphology analysis was conducted using a JEOL JEM 6700 Field Emission Scanning Electron Microscope (FE SEM). TEM images were captured using a JEOL 2010 TEM operating at 200 kV. X-ray photoelectron spectroscopy (XPS) was performed on a Thermo Scientific (Model No ESCALAB 250Xi). UV-Visible spectra were recorded out using UV−Vis spectrophotometer (Model Shimadzu-UV 2401 PC). Steady state photoluminescence spectra were recorded on a Spectrofluorimeter (Hitachi F-7100). Zeta potentials were recorded using Malvern Zetasizer Pro. The electrochemical experiments were conducted using a computer-controlled electrochemical workstation (BioLogic 150e) within a standard three-electrode system. The intermediates of TC degradation were monitored by liquid chromatography-mass spectrometer (Agilent Model 1100).

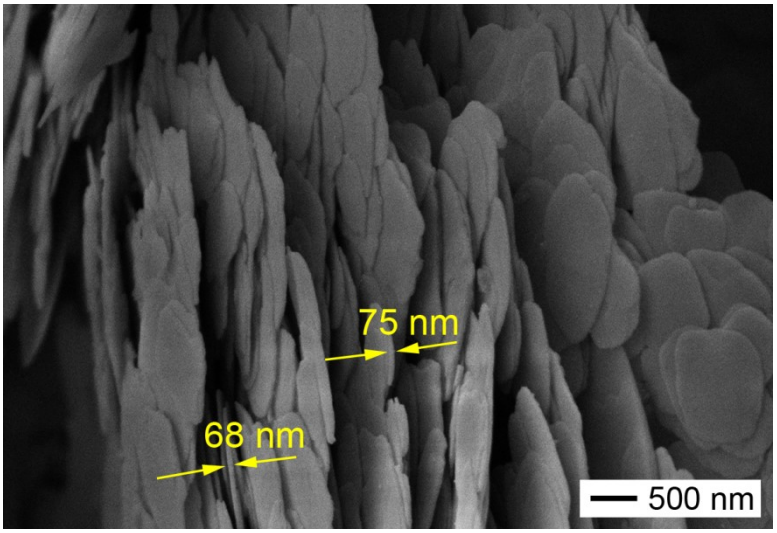

Fig. S1. SEM image of BiOCl nanosheets.

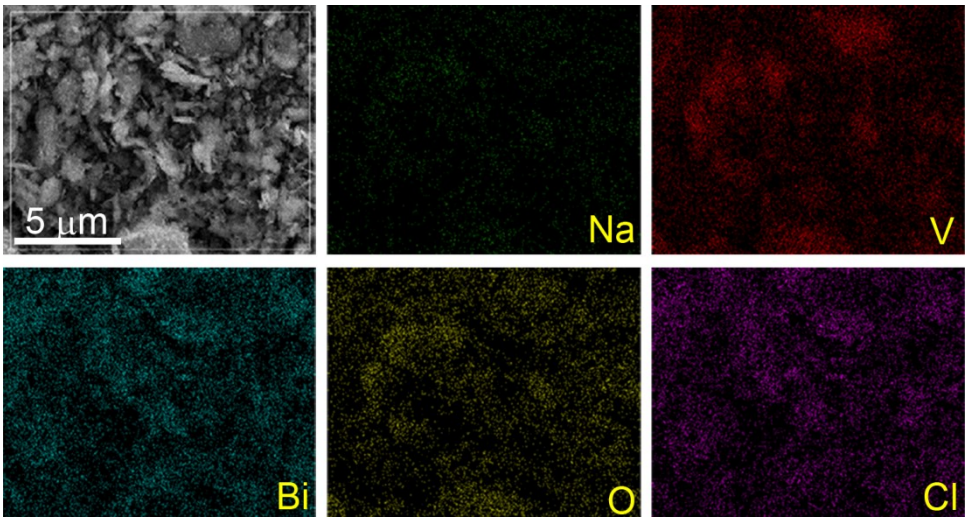

Fig. S2. SEM elemental maps of NaV2O5/BiOCl nanocomposite.

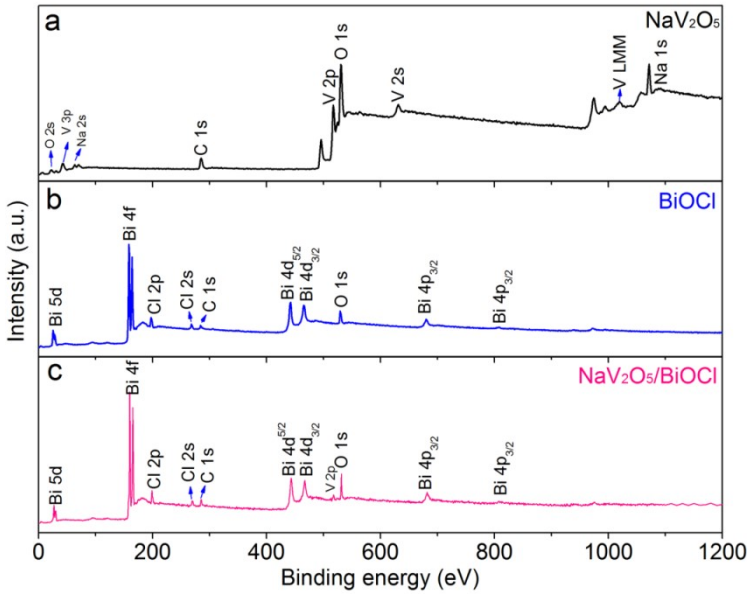

Fig. S3. Survey XPS profile of a) NaV_2O_5, b) BiOCl and c) NaV_2O_5/BiOCl nanocomposite.

Table S1: Summery of XPS analysis of NaV2O5, BiOCl and NaV2O5/BiOCl nanocomposite.

Materials	Peak Position (eV)	Peak Position (eV)	Peak Position (eV)	Peak Position (eV)
	V^{4+} $2p_{3/2}$	**V^{4+} $2p_{1/2}$**	**V^{5+} $2p_{3/2}$**	**V^{5+} $2p_{1/2}$**
NaV_2O_5	516.23 eV	523.13 eV	517.58 eV	524.72 eV
NaV_2O_5/BiOCl	515.78 eV	522.49 eV	516.89 eV	523.86 eV
	$Bi^{3+}4f_{5/2}$	**$Bi^{3+}4f_{3/2}$**		
BiOCl	158.45 eV	163.78 eV		
NaV_2O_5/BiOCl	158.81 eV	164.11 eV		
	Cl $2p_{3/2}$	**Cl $2p_{1/2}$**		
BiOCl	197.46 eV	199.06 eV		
NaV_2O_5/BiOCl	197.72 eV	199.29 eV		
	M-O_L	**M-OH**		
NaV_2O_5	530.14 eV	531.09 eV		
BiOCl	529.61 eV	530.93 eV		
NaV_2O_5/BiOCl	529.87 eV	530.98 eV		

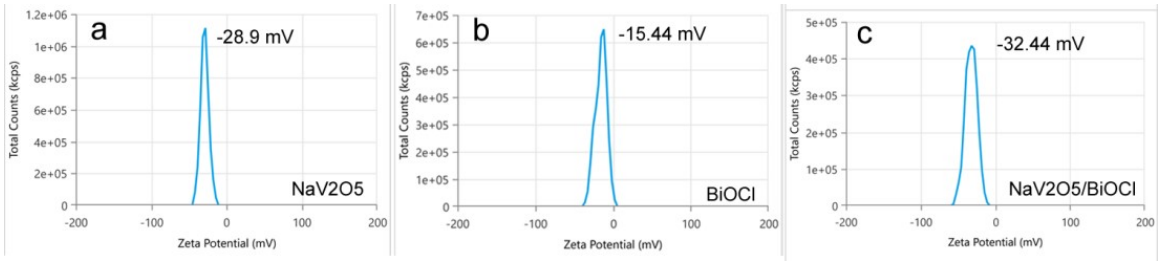

Fig. S4. Zeta potentials measurement of a) NaV2O5, b) BiOCl and c) NaV2O5/BiOCl nanocomposite.

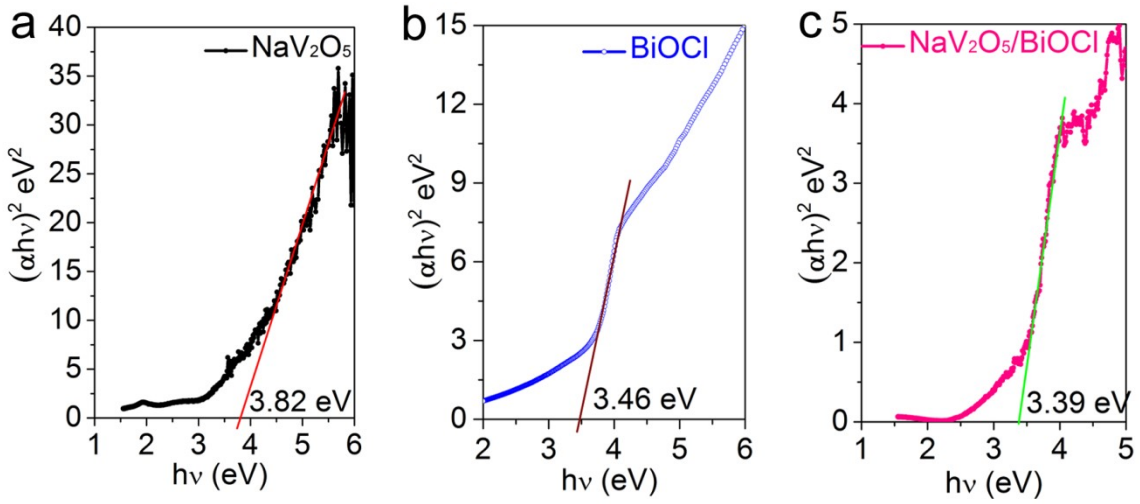

Fig. S5. Band gap energy of a) NaV_2O_5, b) BiOCl and c) NaV_2O_5/BiOCl nanocomposite.

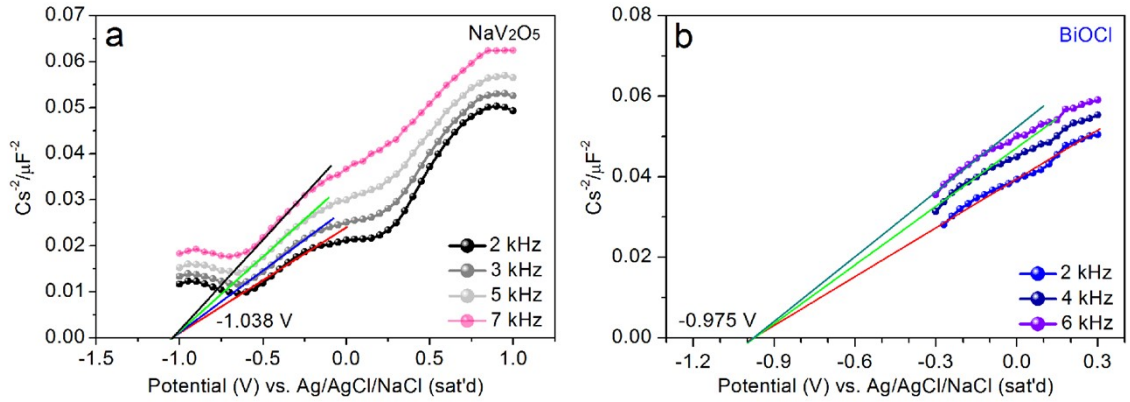

Fig. S6. Mott−Schottky plots of a) NaV_2O_5, and b) BiOCl.

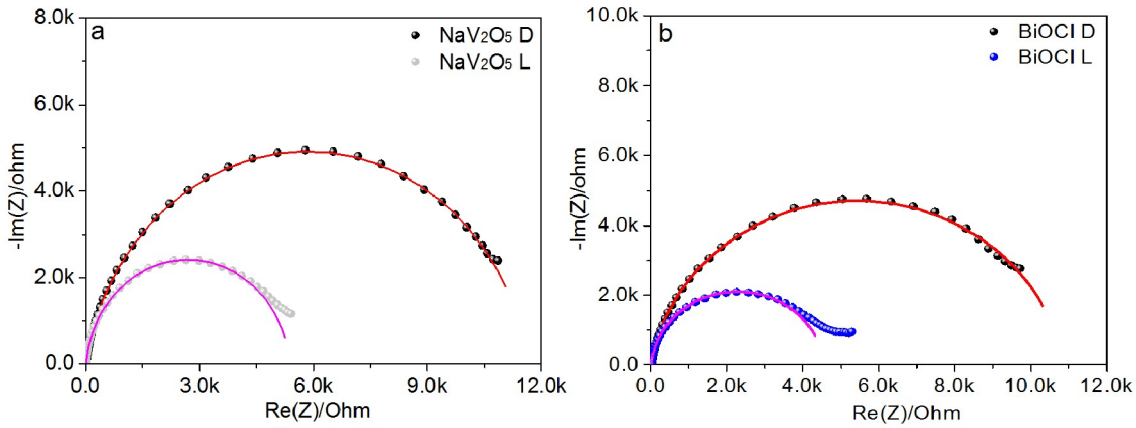

Fig. S7. EIS Nyquist plots for a) NaV_2O_5, and b) BiOCl in the presence and absence of light (300 W Xe lamp).

Table S2. Photoelectrochemical characterization of NaV_2O_5, BiOCl and NaV_2O_5/BiOCl nanocomposite, was obtained from the Nyquist Plot in 0.5(M) Na_2SO_4

Sample	Condition	Electrolyte resistance (R1) (Ohm)	Charge Transfer Resistance (R2) (Ohm)	Constant Phase Elements (Q) [F.s^(a - 1)]
BiOCl/FTO	Dark	19.10	10828	11.89e-6
	Light	13.77	4547	11.49e-6
NaV_2O_5/FTO	Dark	10.70	11662	12.62e-6
	Light	8.01	5379	12.23e-6
NaV_2O_5/BiOCl/ FTO	Dark	13.72	4306	11.86e-6
	Light	13.63	3437	12.46e-6

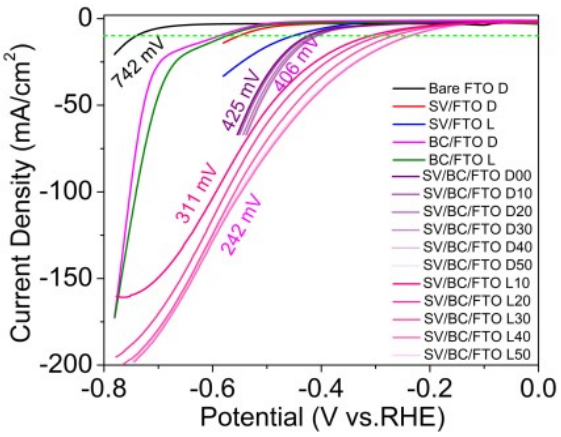

Fig. S8. Linear sweep voltammetry (LSV) curves of HER in 1 M KOH in the presence and absence of light (300 W Xe lamp) for FTO, NaV2O5/NF (SV/FTO), BiOCl/FTO (BC/FTO), and NaV2O5/BiOCl/FTO (SV/BC/FTO).

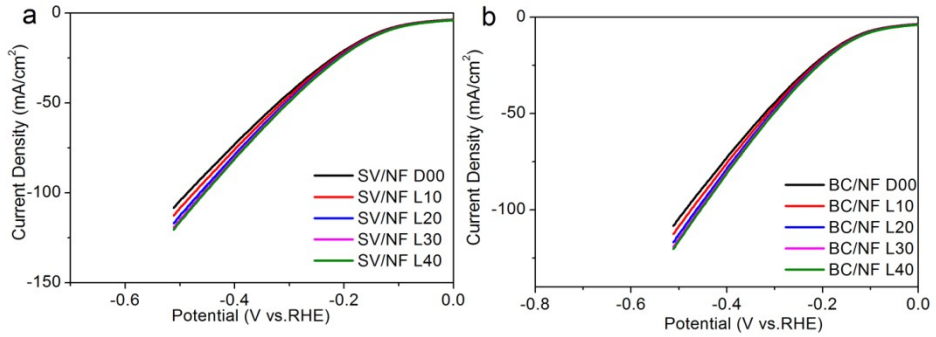

Fig. S9. HER LSV curves for a) NaV_2O_5 and b) BiOCl under light irradiation.

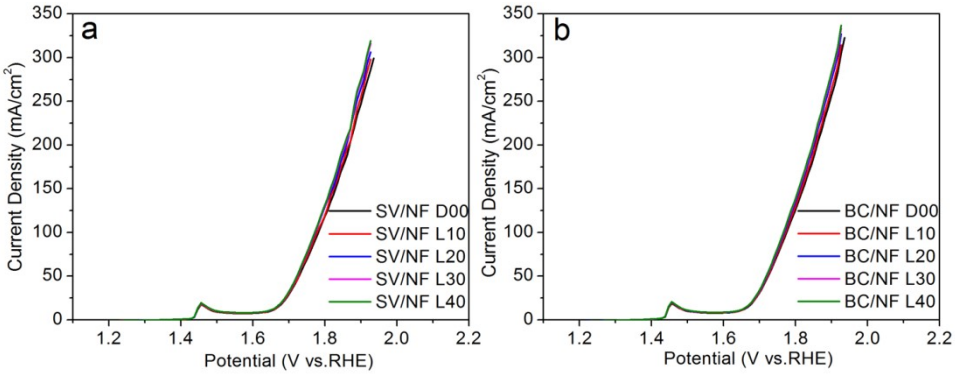

Fig. S10. OER LSV curves for a) NaV_2O_5 and b) BiOCl under light irradiation

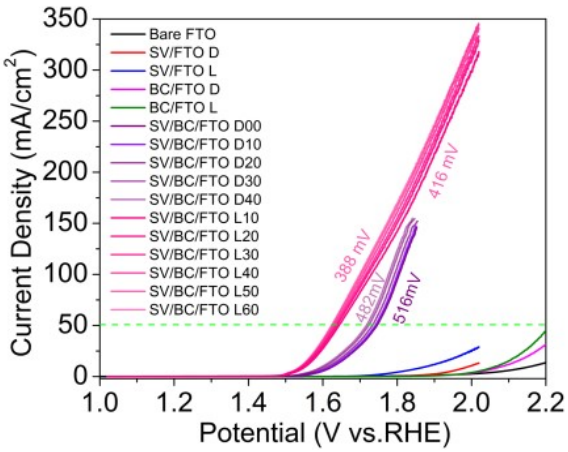

Fig. S11. Linear sweep voltammetry (LSV) curves of OER in 1 M KOH in the presence and absence of light (300 W Xe lamp) for FTO, NaV2O5/NF (SV/FTO), BiOCl/FTO (BC/FTO), and NaV2O5/BiOCl/FTO (SV/BC/FTO).

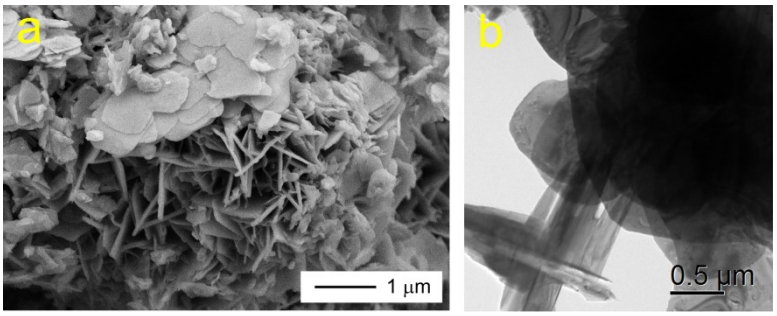

Fig. S12. a) SEM and b) TEM image of the NaV2O5/BiOCl nanocomosite after OER analysis (after 12 hrs).

Table S3. Photoelectrochemical characterization data was obtained from the Nyquist fitted Plot in 1 (M) KOH

Sample	Condition	Electrolyte resistance (R1) (Ohm)	Charge Transfer Resistance (R2) (Ohm)	Constant Phase Elements (Q)
NaV_2O_5/BiOCl/ NF (0.8V)	OER/Dark	6.054	3.167	0.087 88 F.s^(a - 1)
	OER/Light	5.939	2.740	0.090 22 F.s^(a - 1)
NaV_2O_5/BiOCl/ NF (-1.2V)	HER/Dark	1.486	3.451	2.204e-3 F.s^(a - 1)
	HER/Light	1.387	2.315	2.503e-3 F.s^(a - 1)

Table S4. Comparative electrochemical analysis for double layer capacitance (C_{dl}) and corresponding electrochemical active surface area (ECSA) measurement for Ni Foam (NF) supported NaV_2O_5, BiOCl and NaV_2O_5/BiOCl nanocomposite.

$$ECSA = \text{Geometrical Surface area} \times (C_{dl}/C_s)$$

Where C_s represent the capacitance of the flat electrode surface ($Cs = 0.04\ mF/cm^2$).

Sample	**Slope (F/cm^2)**	**C_{dl} (F/cm^2)**	**C_{dl} (mF/cm^2)**	**ECSA (cm^2)**
Bare NF	0.00779 ± 2.04692E-4	0.00389	3.895	97.375
NaV_2O_5/NF	0.01174±6.72309E-4	0.00587	5.870	146.75
BiOCl/NF	0.01104 ± 4.58755E-4	0.00552	5.520	138.00
NaV_2O_5/BiOCl/NF	0.01264 ± 5.10743E-4	0.00632	6.320	158.00

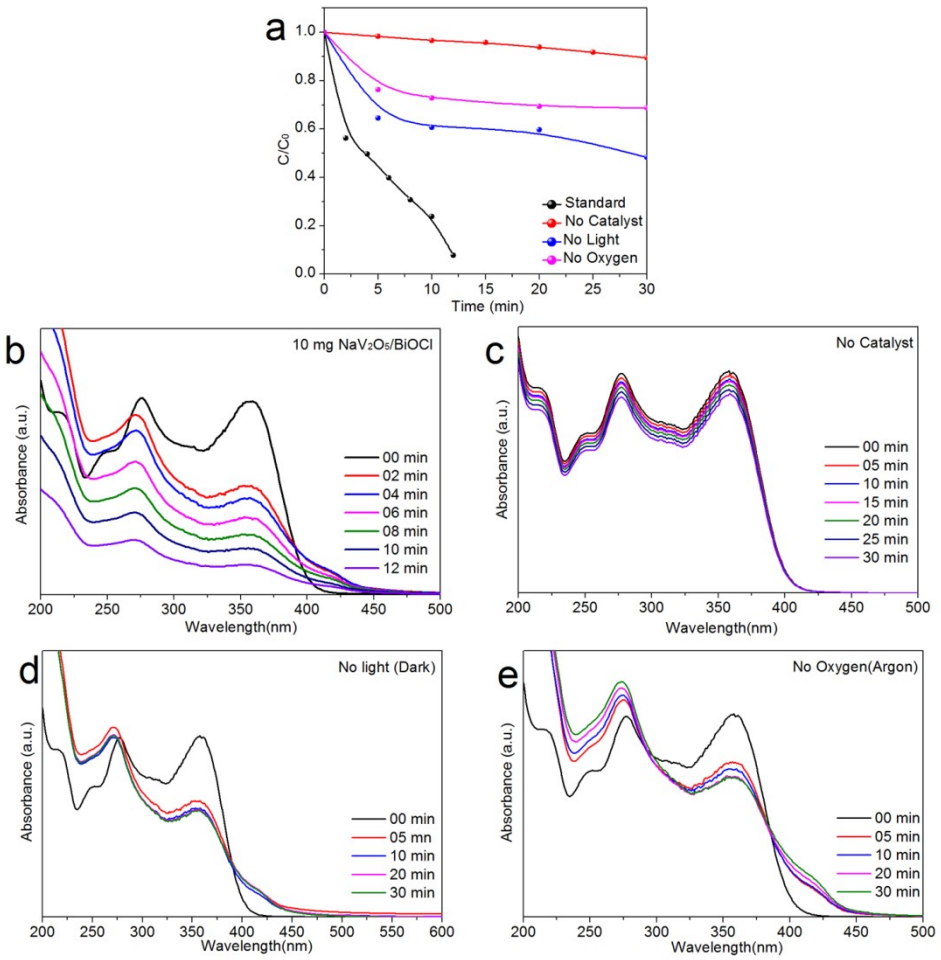

Fig. S13. a) Kinetics plots. b) TC degradation profile at standard condition. TC degradation in different reaction condition c) No catalyst, d) No light (dark) and e) No oxygen (Argon).

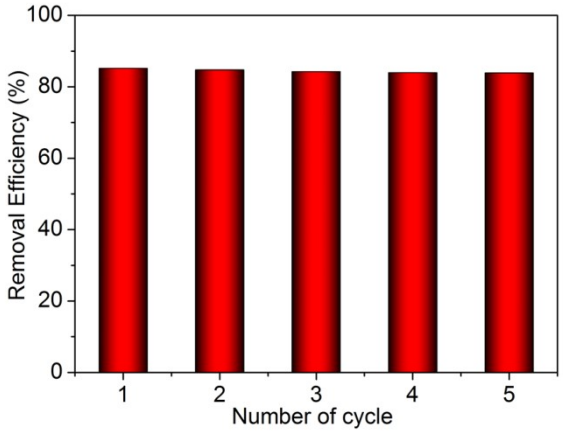

Fig. S14. Recycling efficiency of NaV_2O_5/BiOCl for the TC degradation in white light irradiation.

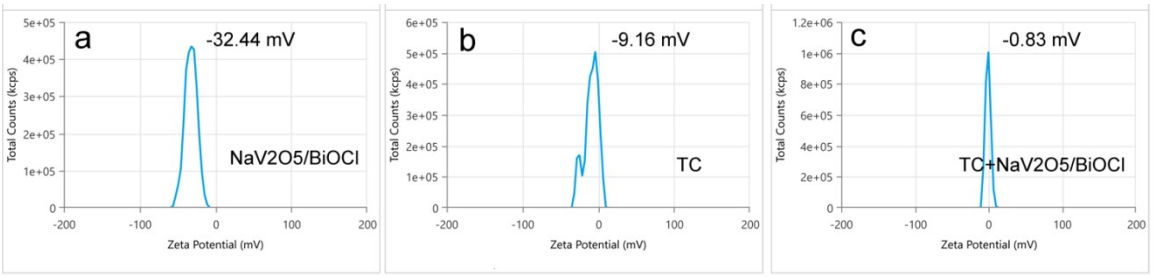

Fig. S15. Zeta potentials measurement of a) NaV_2O_5/BiOCl, b) TC and c) TC with NaV_2O_5/BiOCl in aqueous solution.

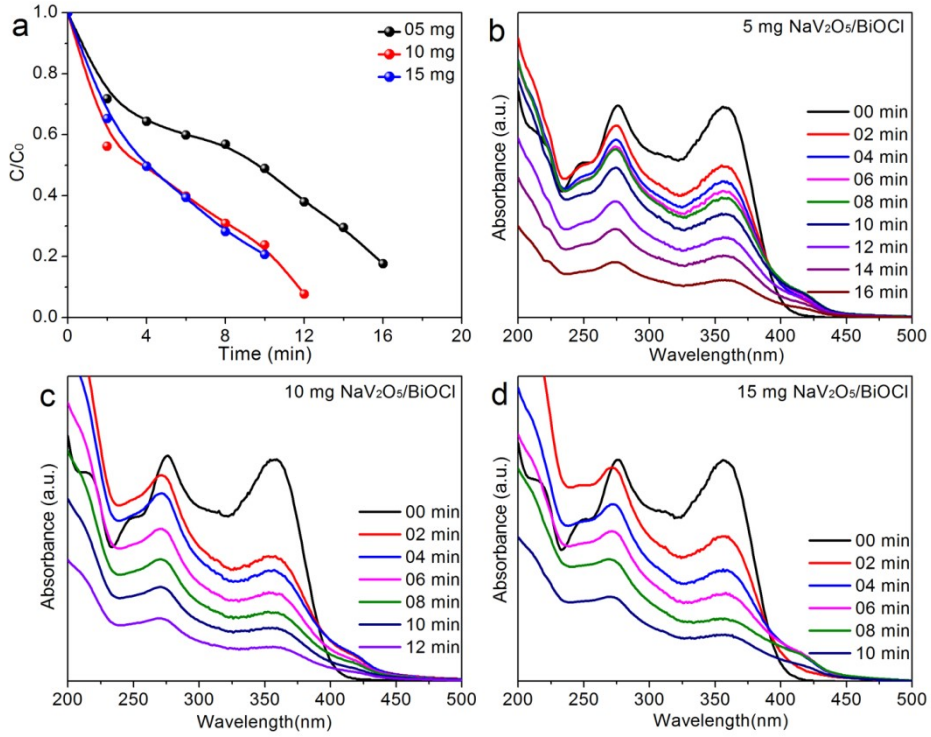

Fig. S16. Effect of catalyst amount. a) Kinetics plots of TC degradation in different catalyst amount. TC degradation profile in different NaV_2O_5/BiOCl catalyst amount b) 5 mg, c) 10 mg, and d) 15 mg.

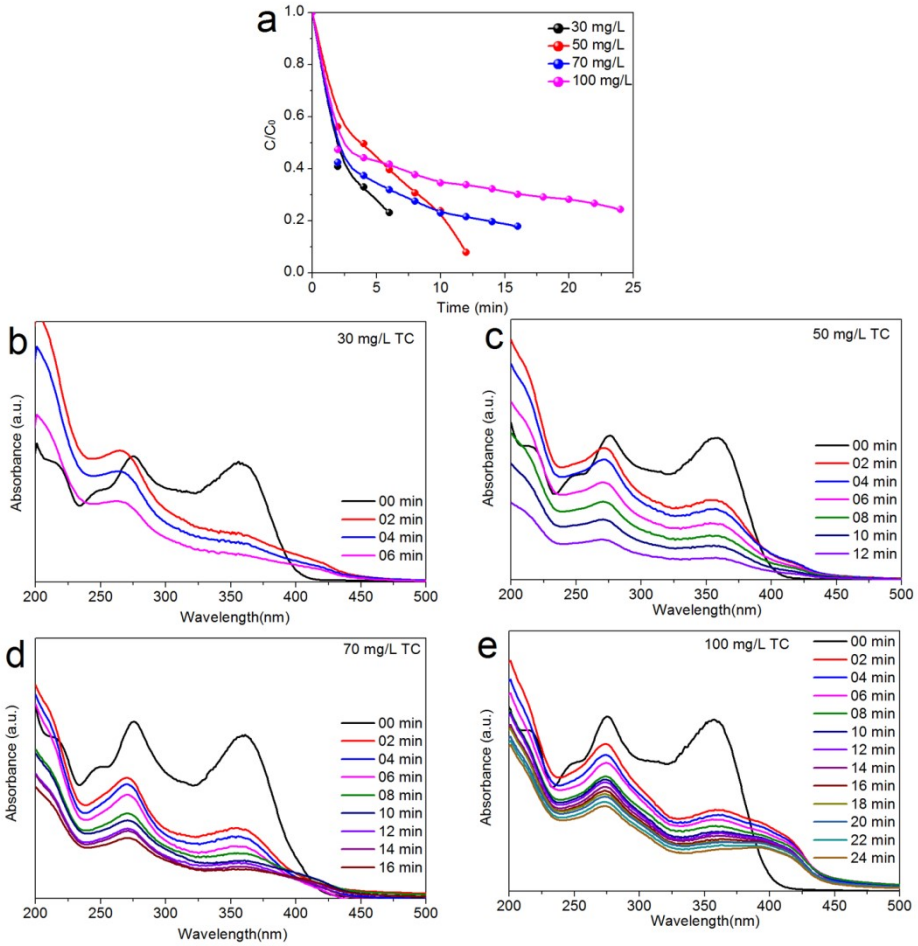

Fig. S17. Effect of TC concentration. a) Kinetics plots of TC degradation in different concentration. TC degradation profile in different TC concentration b) 30 mg/L, c) 50 mg/L, d) 70 mg/L and e) 100 mg/L.

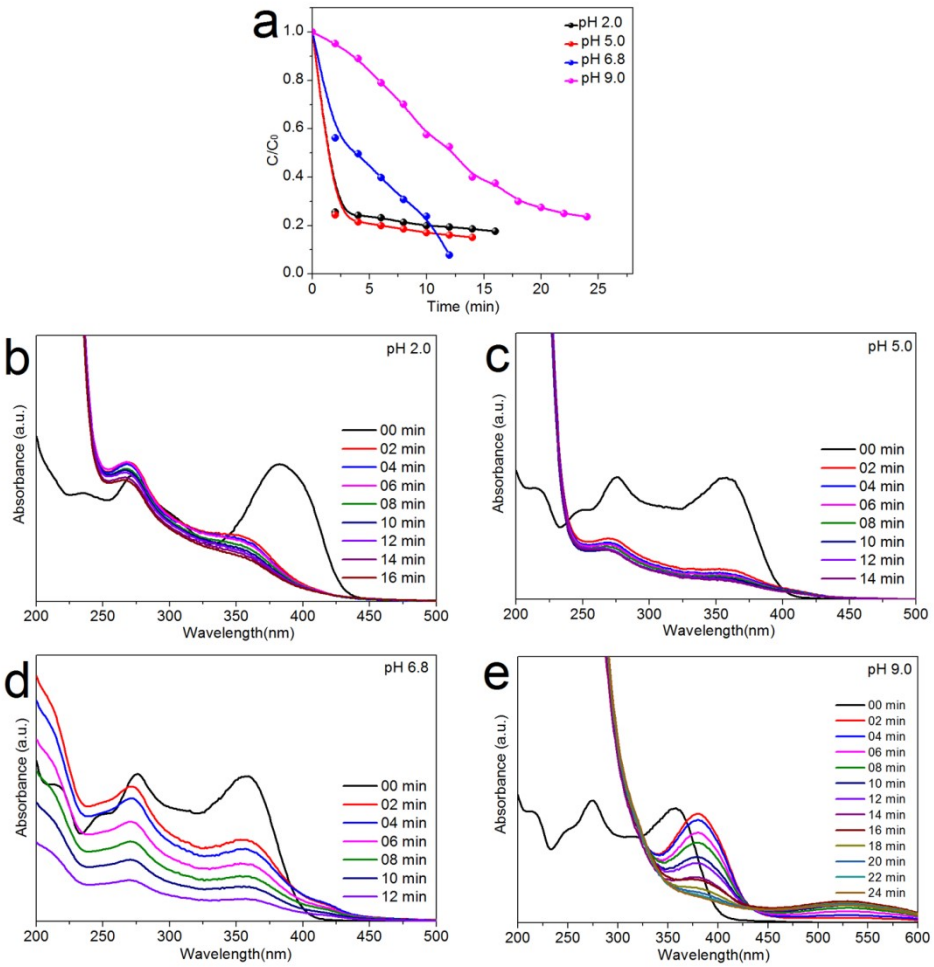

Fig. S18. Effect of pH of the solution. a) Kinetics plots of TC degradation in different pH. TC degradation profile in different pH b) pH=2, c) pH=5, d) pH=6.8 and e) pH=9.

Table S5: NaV2O5/BiOCl nanocomposite for photocatalytic TC degradation in different condition.

Sr No	Variation from standard condition	Time (h)	AQY x 10^6			Average AQY x 10^6	SD
			Expt 1	Expt 2	Expt 3		
1	Standard	0.2	547.0587	534.3015	550.2430	543.8677	8.4362
2	30 mg/L TC	0.1	534.7265	525.2793	525.2793	529.7282	4.7475
3	50 mg/L TC	0.2	547.0587	534.3015	550.2430	543.8677	8.4362
4	70 mg/L TC	0.27	523.7680	513.9237	513.9237	519.7450	5.1626
5	100 mg/L TC	0.4	419.6301	408.2005	425.1317	417.6541	8.6368
6	5 mg catalyst	0.27	354.0541	351.7096	346.1787	350.6475	4.0436
7	10 mg catalyst	0.2	547.0587	534.3015	550.2430	543.8677	8.4362
8	15 mg catalyst	0.16	699.3404	687.1638	698.2256	694.9098	6.7312
9	pH 2.0	0.266	359.4652	357.9017	352.8597	356.7421	3.4524
10	pH 5.0	0.233	422.9244	419.6250	409.3668	417.3054	7.0705
11	pH 6.8	0.2	547.0587	534.3015	550.2430	543.8677	8.4362
12	pH 9.0	0.4	221.5846	219.3343	220.7808	220.5665	1.1404
[a]Standard conditions: NaV2O5/BiOCl Catalyst (10 mg), TC Solution (30 mL, 50 mg/L), 1 atm O_2, 300 Watt Xe Lamp (100 $mWcm^{-2}$), Room temperature (25 °C). SD-Standard Deviation							

Averages and Standard Deviations were calculated based on the below formula.

Mean value $\bar{x} = \sum_{i=1}^{n} x_i/N$ ……(a)

The standard deviation $\sigma_x = \sqrt{\sum (x_i - \bar{x})^2/(N-1)}$ ……(b)

Where x_i are the values from the individual measurements and N is the total number of measurements.

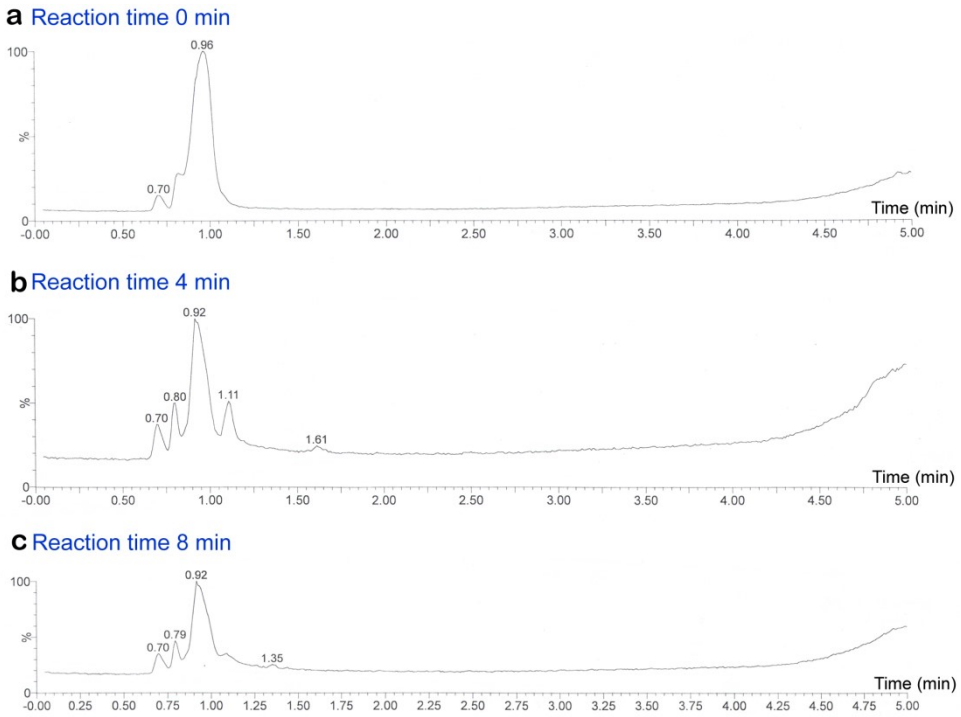

Fig. S19. The liquid chromatography profiles of TC degradation with different intermediate products a) 0 min, b) 4 min, c) 8 min.

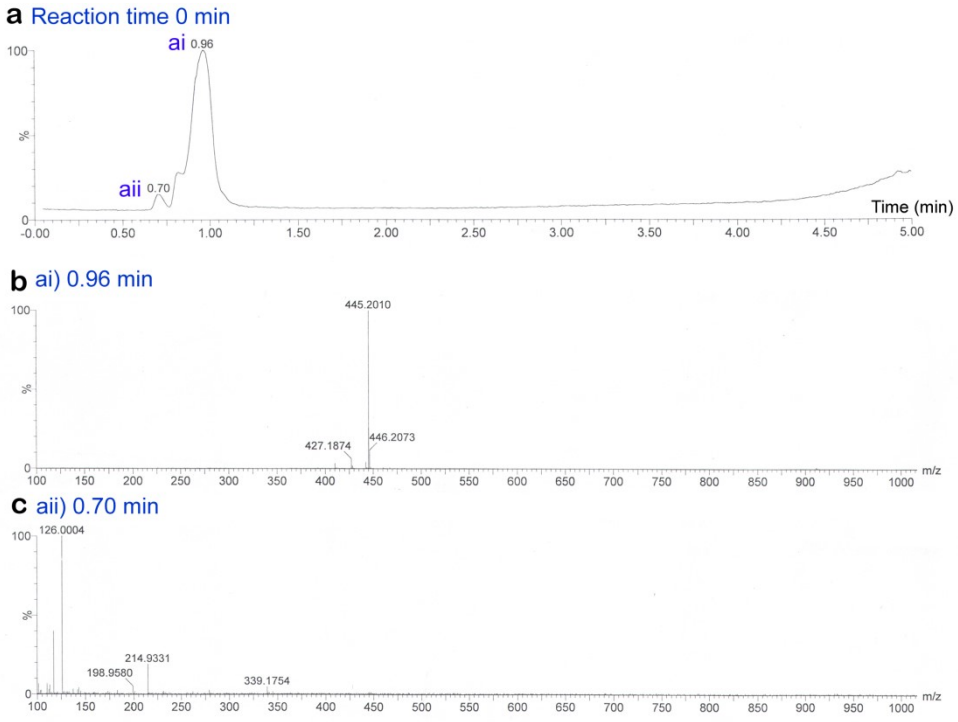

Fig. S20. The liquid chromatography profile and corresponding ESI mass spectra of TC degradation at reaction time 0 min.

Table S6. The information of potential intermediates at 0 min in the TC degradation identified by LC–MS using positive ESI.

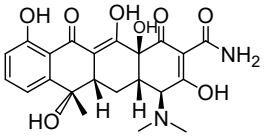 ai) *m/z* 445.19, $C_{22}H_{24}N_2O_8$	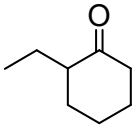 aii) *m/z* 126.00, $C_8H_{14}O$	

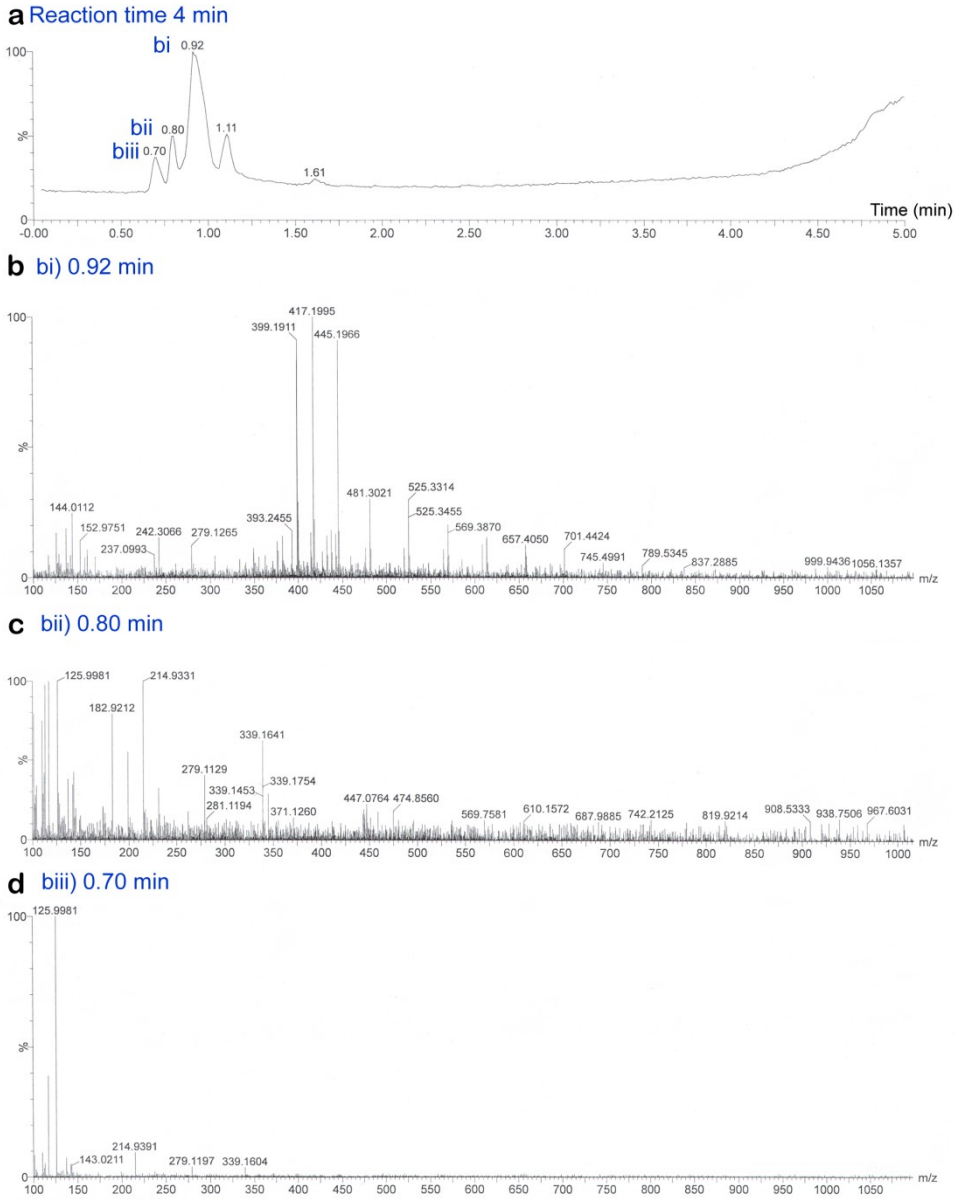

Fig. S21. The liquid chromatography profile and corresponding ESI mass spectra of TC degradation at reaction time 4 min.

Table S7. The information of potential intermediates at 4 min in the TC degradation identified by LC–MS using positive ESI.

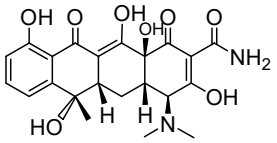 bi) *m/z* 445.19, $C_{22}H_{24}N_2O_8$	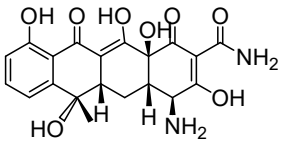 bi) *m/z* 417.19, $C_{20}H_{20}N_2O_8$	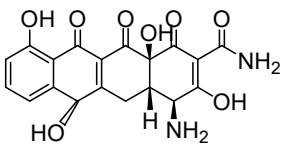 bi) *m/z* 399.19, $C_{19}H_{16}N_2O_8$
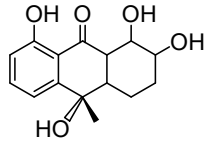 bi) *m/z* 279.12 $C_{15}H_{18}O_5$	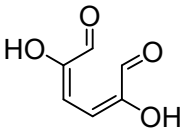 bi) *m/z* 144.01, $C_6H_6O_4$	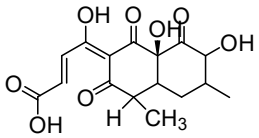 bii) *m/z* 339.16, $C_{16}H_{18}O_8$
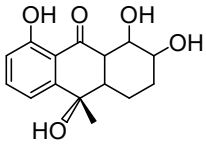 bii) m/z 279.11 $C_{15}H_{18}O_5$	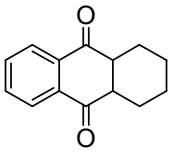 bii) *m/z* 214.93, $C_{14}H_{14}O_2$	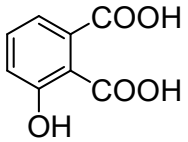 bii) *m/z* 182.92, $C_8H_6O_5$
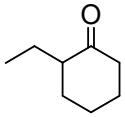 biii) *m/z* 126.00, $C_8H_{14}O$		

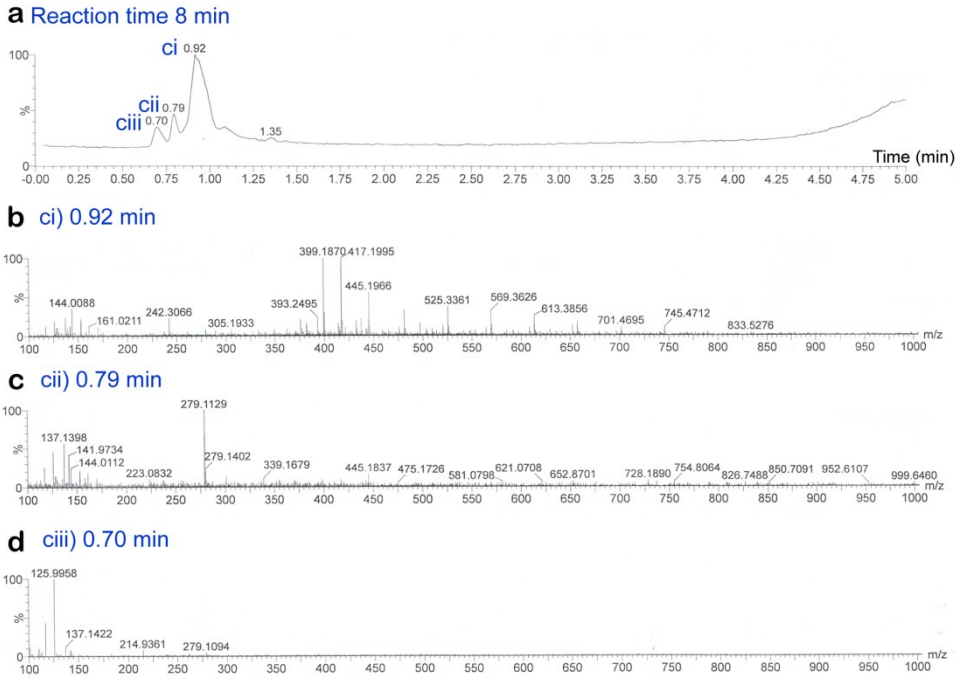

Fig. S22. The liquid chromatography profile and corresponding ESI mass spectra of TC degradation at reaction time 8 min.

Table S8. The information of potential intermediates at 8 min in the TC degradation identified by LC–MS using positive ESI.

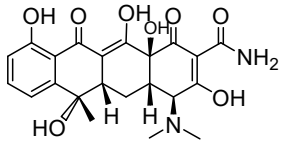 ci) *m/z* 445.19, $C_{22}H_{24}N_2O_8$	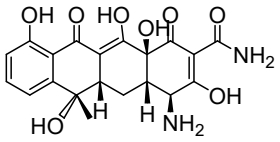 ci) *m/z* 417.19, $C_{20}H_{20}N_2O_8$	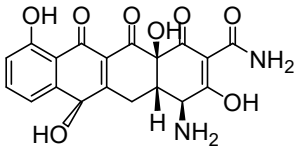 ci) *m/z* 399.19, $C_{19}H_{16}N_2O_8$
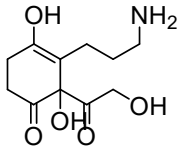 ci) *m/z* 242.30, $C_{11}H_{17}NO_5$	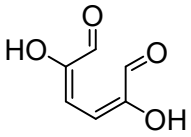 ci) *m/z* 144.00, $C_6H_6O_4$	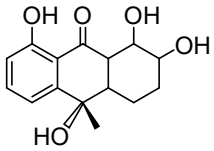 cii) *m/z* 279.11 $C_{15}H_{18}O_5$
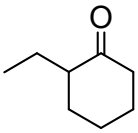 ciii) *m/z* 126.00, $C_8H_{14}O$		

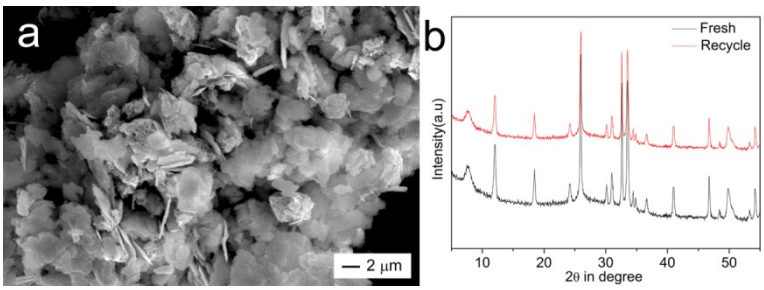

Fig. S23. a) SEM and b) powder XRD analysis of NaV2O5/BiOCl nanocomosite after 3rd cycle of recyclability test.